Food Chemistry: X 23 (2024) 101635

Contents lists available at ScienceDirect

Food Chemistry: X

journal homepage: www.sciencedirect.com/journal/food-chemistry-x

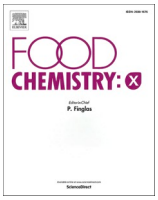

Development and characterization of defatted coconut flour based oleogels: A fat substitute for application in oil-fortified surimi

Xia Gao [a], Zhisheng Pei [b], Xiangzhou Yi [a], Xuan Zhang [a], Dongxue He [a], Zilan Feng [a], Guanghua Xia [a], Xuanri Shen [a,b,*]

[a] Hainan Engineering Research Center of Aquatic Resources Efficient Utilization in South China Sea, Key Laboratory of Seafood Processing of Haikou, School of Food Science and Engineering, Hainan University, Hainan 570228, China
[b] School of Food Science and Engineering, Hainan Tropic Ocean University, Sanya 572022, China

ARTICLE INFO

Keywords:
Network
Rheological
Protein secondary structure
Gel property
Dietary fiber

ABSTRACT

This research examined the impact of defatted coconut flour (DCF)-based oleogels on the quality of surimi. Microscopic analysis indicated that the dietary fiber present in DCF could act as the main structure of the oleogels network. The formation of the oleogels network primarily relies on the tensile intramolecular or intermolecular hydrogen bonds between DCF and corn oil. The oleogels displayed oil binding capacity of up to 96.95% and exhibited favorable mechanical and rheological properties. Efforts were undertaken to integrate the acquired oleogels into silver carp surimi to create oil-fortified surimi products. Adding oleogels significantly enhanced the gel strength, texture, and water-holding capacity of surimi compared to adding corn oil. Especially, oleogels containing 5.0 % (w/v) DCF concentration elevated the lipid content in the surimi and preserved the gel and texture properties. Therefore, incorporating oleogels in surimi presents a potential solution for enhancing the nutritional content of surimi products.

1. Introduction

Surimi products are characterized by a unique taste profile and serve as a valuable source of premium protein, rendering them attractive to consumers (Yi et al., 2023). Rinsing is necessary in the surimi preparation process to improve texture characteristics. Nevertheless, the nutrient loss, including unsaturated fatty acids and fat-soluble vitamins, incurred during the extensive rinsing process in surimi preparation poses a challenge (Bao et al., 2022). It is necessary the to add lipids to address nutritional imbalances. Currently, lipid is predominantly integrated into surimi products through direct addition or as pre-emulsions. The direct addition of liquid oil is found to disrupt hydrogen bonds within myofibrillar protein, impede the development of a cohesive gel network, and result in undesirable textural characteristics (He et al., 2022; Shi et al., 2014). While pre-emulsions can address this issue, it remains insufficient in achieving the desired surimi structure and gel strength due to elevated water content and diminished protein content (Lv et al., 2023, Zhang, Lu, et al., 2023). Hence, developing a technique for integrating oil that enhance the lipid composition of surimi without compromising its overall quality is crucial.

Oleogels is gel-like substances created by encapsulating liquid oil within a three-dimensional network of crystalline particles or polymer structures. (Zheng et al., 2020) The utilization of food-based materials, such as protein and polysaccharide, for forming three-dimensional polymer networks to develop oleogels has garnered increasing interest (Zhang et al., 2021). However, oleogels prepared with a singular protein or polysaccharide may present limitations, including inadequate oil-binding capabilities and vulnerability to oxidation (Li et al., 2022; Sharma et al., 2023; Vélez-Erazo et al., 2022). This phenomenon can be explained by a thin emulsion interfacial layer and a three-dimensional network that is susceptible to collapsing, resulting in oil leakage upon water removal (Tavernier et al., 2017). Protein-polysaccharide complexes, on the other hand, can create a more robust interface layer within the emulsion, thereby improving the physicochemical characteristics of oleogels (Su et al., 2023; Xie et al., 2023). However, at present, the preparation of these complexes depending on remixing and compounding are intricate and expensive processes, which restrict their practical use. Therefore, exploring the potential of utilizing the natural protein-polysaccharide complex as the primary ingredient in oleogels is warranted.

* Corresponding author at: School of Food Science and Engineering, Hainan University, No. 58, Renmin Avenue, Meilan District, Haikou 570228, China.
E-mail address: shenxuanri2009@163.com (X. Shen).

https://doi.org/10.1016/j.fochx.2024.101635
Received 24 April 2024; Received in revised form 14 June 2024; Accepted 6 July 2024
Available online 15 July 2024

Defatted coconut flour (DCF), a residual product of coconut milk and oil extraction, is rich in dietary fiber and protein, along with trace amounts of free amino acids, vitamins, minerals, and other essential micronutrients (Rodsamran & Sothornvit, 2018; Trinidad et al., 2006). Compared to conventional protein-polysaccharide complexes, DCF is easily accessible and cost-effective, making it better suited for extensive food processing. The dietary fiber within DCF demonstrates significant swelling and adsorption capacities, albeit with limited emulsifying abilities. Conversely, the protein component of DCF exhibits strong emulsifying properties, enhancing the interface layer of the dietary fiber emulsion (Trinidad et al., 2006). Consequently, the DCF stabilized emulsion demonstrates the ability to effectively maintain the integrity of the three-dimensional mesh structure and enhance the solidification of oil post-water removal. As a result, DCF shows promise for the production of high-quality oleogels in the realm of food processing. To date, limited attention has been given to the formation mechanism and utilization of DCF-based oleogels in the food sector.

This study employed the emulsion-template method to create DCF emulsions for the oleogels system and investigate the potential application of oleogels in the food industry by integrating them into surimi products. The microscopic morphology and three-dimensional network structure of oleogels were examined through optical microscopy, polarized light microscopy, and X-ray diffraction (XRD). The physical properties were assessed using rheology, texture and oil measurements, and the potential incorporation into surimi was investigated to determine its suitability in the food industry. This research contributes valuable insights for advancing and utilizing of DCF-based oleogels, and offers guidance for novel applications within the realm of food science and technology.

2. Materials and methods

2.1. Materials

Coconuts (*Cocos nucifera* L., 12 months maturity) were obtained from a local market (Haikou, China). Corn oil was purchased from Luhua Co., Ltd. (Dongguan, China). Silver carp surimi (75.18 ± 2.33% moisture) was purchased from Jingli Aquatic Food Co., Ltd. (Honghu, China). Nile red and Nile blue were analytical grade and obtained from Macklin Biochemical Co., Ltd. (Shanghai, China). All other chemical reagents were analytical grades from Guangzhou Chemical Reagent Factory (Guangzhou, China).

2.2. Preparation of defatted coconut flour (DCF)

The grated coconut meat (1000 g) was freeze-dried and ground into a fine powder. The powder was degreased with hexane at a ratio of 1:10 (w/v) and stirred at 25 °C for 2 h. Subsequently, the defatted flour was left to stand for 12 h at 25 °C under a hood to allow the solvents to evaporate. DCF was then stored at 4 °C. The main components of DCF were dietary fiber (60.86 ± 4.36 g/100 g) and protein (10.80 ± 0.31 g/100 g), with the content of other components shown in **Table S1.**

2.3. Preparation of oleogels

Following the methods reported by Keshanidokht et al. (2023), DCF at concentrations of 2.5%, 5.0%, 7.5%, 10.0%, and 12.5% (w/w) was completely dissolved in MilliQ water at 4 °C and stirred for 12 h. The DCF solution was mixed with corn oil at a ratio of 1:1 (v/v) and then homogenized at 7000 rpm for 2 min using a high-speed homogenizer (XHF-DY, Scientz, Ningbo, China) to obtain the emulsion. The emulsion was then dried by a freeze dryer (LGJ–12 A, Beijing Sihuan Scientific Instrument Factory Company, Beijing, China). Then, the dried product was sheared at 800 rpm for 20 s to obtain oleogels, named as OD2.5, OD5.0, OD7.5, OD10.0, OD12.5, respectively.

2.4. Characterization of emulsion and oleogels

2.4.1. Microscopic observation

During emulsion preparation, Fluorescent Brightener (0.01%, w/v), Nile Red (0.01%, w/v) and Nile Blue (0.01%, w/v) were added to dye dietary fiber, corn oil, and protein, respectively. Subsequently, microscopic images of the emulsions were obtained using a confocal laser scanning microscope (CLSM, FV3000, Olympus, Tokyo, Japan) at an excitation wavelength of 365 nm (Fluorescent Brightener), 488 nm (Nile Red) and 633 nm (Nile Blue) at 25 °C.

The oleogels' appearance was captured using a digital camera (Alpha 7 II, Sony, Tokyo, Japan). Trinocular polarizing microscope (PLM) images for oleogels were captured using a trinocular transflective polarizing microscope MP30 (Guangzhou Mingmei Optoelectronic Technology Co., Ltd., Guangzhou, China) at 100x magnification.

2.4.2. Measurement of XRD

The structural properties of oleogels was examined using an X-ray diffractometer (Smartlab SE, Rigaku corporation, chengshi Japan) with a Cu liquid X-ray radiation source. The diffraction angle ranged from 5° to 40° (2θ), and the scanning speed was set at 1 step/min, 25 °C.

2.4.3. Measurement of attenuates total reflection Fourier transform infrared spectroscopy (ATR-FTIR)

The infrared spectra of the oleogels were recorded at 25 °C using a FTIR spectrometer (ALPHA II, Bruker, Germany). In brief, the oleogels and potassium bromide were thoroughly mixed at a mass ratio of 1:100 and ground in an agate mortar, followed by compression using a tablet press. Spectra were measured across wavenumbers ranging from 4000 to 400 cm^{-1} with a resolution of 2 cm^{-1}.

2.4.4. Measurement of oil binding capacity (OBC)

Oleogels were placed into a tube for the centrifugation (Z326/Z326K, Maschinenfabrik Berthold Hermle AG, Gosheim, Germany) at 10,000 rpm for 15 min at 25 °C. The spilled oil was poured out, and the centrifuge tube containing the remaining oleogels was weighed (Jiang et al., 2022). OBC (%) was calculated using Eq. (1):

$$OBC(\%) = \frac{m_2 - m_0}{m_1} \times 100 \quad (1)$$

where m_0, m_1, and m_2 represent the weight of centrifuge tube, the weight of the oleogels, and the weight of the centrifuge tube with the removed oil after centrifugation, respectively.

2.4.5. Measurement of rheological properties

The rheological properties of oleogels were tested using an MCR 92 rotational rheometer (Anton Paar, Austria) equipped with a Peltier system. Frequency sweep tests were performed at frequencies ranging from 0.1 to 100 Hz at 0.1% strain. Apparent viscosity was obtained at shear rates ranging from 0.1 s^{-1} to 100 s^{-1}. Amplitude sweeps of all samples were measured by strain sweep tests (0.1–100%) at a frequency of 1.0 Hz. Thixotropy was evaluated by time sweep tests while varying the shear rates.

2.5. Preparation of surimi

According to our previous method (Pei et al., 2023), sodium chloride (3% was added to 100 g silver carp surimi and mixed using a food processor (UMC5, STEPHAN Universal Machine, Germany) for 1 min. Subsequently, 20% (w/w) corn oil or oleogels with different DCF concentrations were added, labeled as "CO group","OD2.5 group", "OD5.0 group", "OD7.5 group", "OD10.0 group", and "OD12.5 group", respectively, and mixed for 4 min. The surimi samples were then loaded into polyvinyl dichloride bag casings and heated at 40 °C for 40 min, followed by steaming at 90 °C for 30 min. After heating, the samples were

cooled in ice water to 25 °C and then refrigerated at 4 ± 2 °C. The surimi without oleogels was used as a control.

2.6. Measurement of surimi quality

2.6.1. Measurement of texture profile analysis (TPA) and gel strength

The TPA and gel strength of samples were measured using a texture analyzer (TMS-PRO, FTC Co., USA) (He et al., 2022). Each sample (20 mm diameter × 20 mm height) was tested at a speed of 60 mm/min and 15 mm of compression distance with a 0.2 N trigger force. The measurement was repeated 6 times for each sample.

2.6.2. Measurement of water holding capacity (WHC) of surimi

The WHC of surimi was determined following the methods of Bao et al. (2022). The samples were weighted (W_0) and then centrifuged at 10,000 rpm (25 °C, 10 min). After weighting the sample after centrifugation (W_1), the WHC (%) was calculated according to Eq. (2):

$$\text{WHC}\ (\%) = \frac{W1}{W0} \times 100 \tag{2}$$

2.6.3. Measurement of water distribution of surimi

The water distribution of surimi was determined using a low field nuclear magnetic resonance (LF-NMR) analyzer (NMI20-060H-I Newmag Co., Suzhou, China). T2 spectrum was determined utilizing Carr-Purcell-Meibom-Gill (CPMG) sequence at a proton resonance frequency of 22.0 MHz. Proton density imaging of surimi was measured by multi-spin echo imaging sequences on a magnetic resonance imager (MRI). Grayscale images were processed using OsiriX software (Niumag Analytical Instrument Co., Suzhou, China).

2.6.4. Measurement of rheological properties of surimi

Using a rheometer (MCR 92, Anton Paar, Austria) equipped with a plate gripper (PP50), the changes in the elastic modulus (G') and viscous modulus (G") of surimi during heating were conducted by temperature sweeps. Samples were heated from 20 °C to 90 °C at a speed of 1 °C/min, a frequency of 1 Hz and strain of 1%.

2.6.5. Measurement of microstructure of surimi

To study the dispersion and aggregation behavior of oil droplets in surimi, surimi was fixed in 4% (w/v) paraformaldehyde and dehydrated with 30% (w/v) sucrose solution at 4 °C. The surimi was then cut into 8–10 μm flakes using a cryomicrotome following the method of He et al. (2022). The flakes were subsequently immersed in 60% (v/v) isopropanol, stained with 0.5% (w/v) Oil Red O (ORO) dye solution for 15 min, and washed with 75% (v/v) alcohol. The flakes were placed on coverslips and observed under a 400 x microscope (Ti—S, Nikon, Tokyo, Japan).

The microscopic morphology of surimi was analyzed using a scanning electron microscope (SEM, JEOL JSM-5800 LV, Tokyo, Japan). The samples (3 mm × 3 mm × 3 mm) were fixed in 2.5% glutaraldehyde for 24 h. They were then washed with phosphate buffer for 15 min, and dehydrated with graded ethanol for 10 min. Subsequently, the samples were vacuum freeze-dried. The surface topography of the sample was checked by SEM at 15 kV, and all images were recorded at 500 x magnification.

2.6.6. Measurement of chemical forces of surimi

The following solutions were prepared: 0.05 mol/L NaCl solution (S1), 0.6 mol/L NaCl solution (S2), a mixture of 0.6 mol/L NaCl and 1.5 mol/L urea (S3), and a mixture of 0.6 mol/L NaCl and 8.0 mol/L urea (S4). Samples were mixed with of the above solution (1:5 v/v) and homogenized at 8000 rpm for 2 min. Subsequently, the solution was centrifuged (10,000 rpm, 4 °C, 20 min), and the protein concentration in the supernatant was determined. Chemical forces, including ionic bonds (S2-S1), hydrogen bonds (S3-S2), and hydrophobic interactions (S4-S3), were calculated.

2.6.7. Measurement of Raman spectrum of surimi

The samples were tested using a DXR2 laser Raman microscopy analyzer (DXR2, Thermo Fisher Scientific, USA). The spectra were collected across the wavenumber from 500 to 3500 cm^{-1}.

2.7. Statistical analysis

All experiments were performed in at least triplicate, and the average values were reported. Significance differences ($p < 0.05$) were analyzed using analysis of variance (ANOVA) and Duncan's multiple range tests by using SPSS software (SPSS Inc., Chicago, USA).

3. Results and discussion

3.1. Characterization of oleogels

3.1.1. Micromorphology of oleogels

To understand the formation of the oleogels network, CLSM was employed to observe the distribution of oil and water phases in the emulsion (Fig. 1A). In the CLSM image, blue, red, and green colors represented dietary fiber, protein, and oil, respectively. The images revealed densely packed and uniformly distributed oil droplets in the emulsions. Dietary fiber and protein accumulated around the droplets, forming a dense interfacial barrier. Dietary fiber form the main structural framework around the oil droplets, attributed to their role as emulsifiers and thickeners (Su et al., 2023). Furthermore, with increasing DCF concentration, droplet size gradually decreased, leading to a denser network structure due to spatial repulsion between droplets (Liao et al., 2024). Thus, upon removal of water from the emulsion, the mesh structure may form a thick and hard shell on the oil droplet surface, effectively structuring the oil.

The apparent morphology of the oleogels formed by freeze-drying of the emulsion is depicted in Fig. 1B. The appearance of the oleogels varies with the concentration of DCF, giving them a yellowish and solid texture. With increasing DCF concentration, the texture of the oleogels becomes rougher and harder, with a less oily appearance. Oleogels with lower DCF concentrations (2.5–5.0% w/v) exhibit a homogeneous paste-like texture, exhibiting slight phase separation behavior. The loose network structure of the emulsion, which partially collapses after dehumidification, leads to oil leakage.

PLM observation provided insight into the effect of DCF concentration on oleogels network formation (Fig. 1C), further confirming that dietary fiber is a rigid support for the internal structure of the oleogels. A loose fibrous network is observed at DCF concentrations of 2.5–7.5% (w/v), with oil droplets dispersed between irregularly shaped fiber. In contrast, oleogels with higher concentrations of DCF exhibited a denser and more ordered particle structure, which may be due to the molecular entanglement of dietary fiber, resulting in aggregate formation (Li et al., 2023). Birefringence domains inside and between the fiber particles are visible, indicating the formation of an organized crystal or fiber network. This microstructure contributes to the enhancement of hardness and gel properties of the oleogels.

The microscopic results of oleogels revealed that DCF facilitated the recombination of dietary fiber into an interconnected gel network that entrapped oil through steric site blockade and thickening.

3.1.2. XRD analysis of oleogels

XRD analysis examined the crystalline structure of DCF and oleogels (Fig. 2A). DCF exhibited a semi-crystalline pattern with a broad peak at 20.4° (2θ), indicating an ordered arrangement of fiber or protein (Tan et al., 2023). The oleogels produced similar peaks at 20.5°(2θ) but narrower and stronger, indicating that the dietary fiber molecular chains in the DCF underwent a conformational change in forming the gel network structure. In the emulsion system used for oleogels preparation,

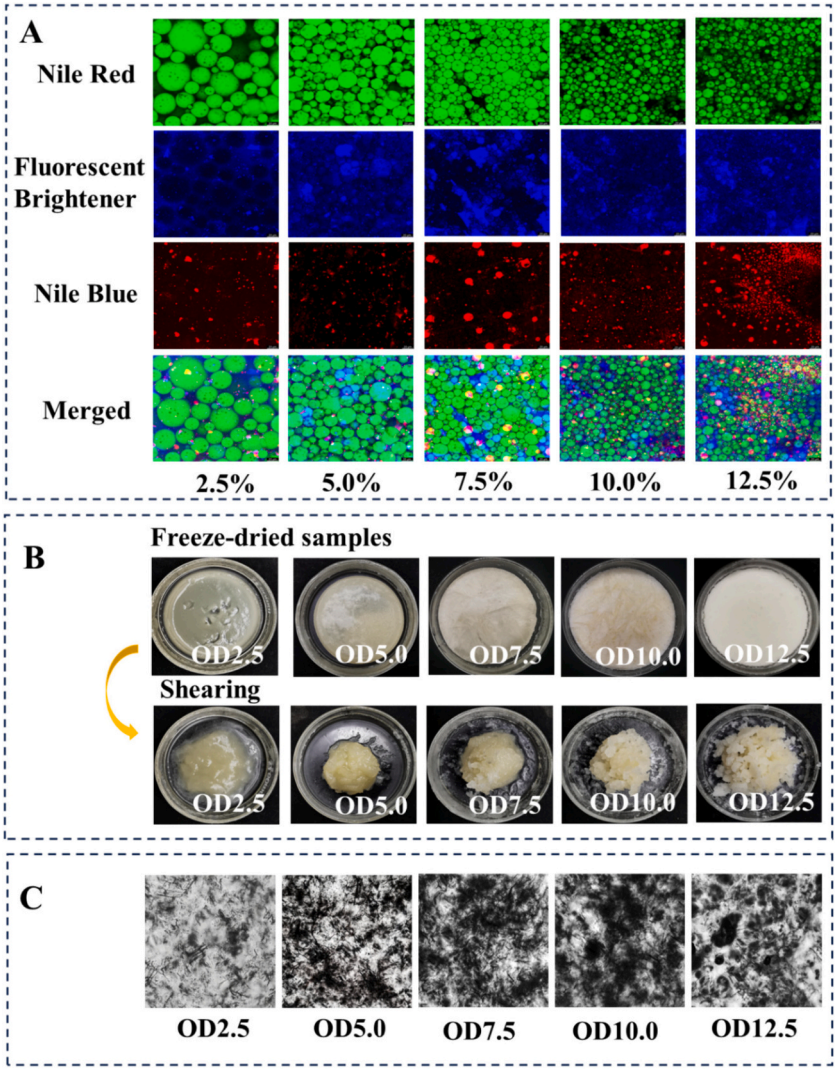

Fig. 1. The morphology of emulsions and DCF-based oleogels with different DCF concentrations: (A) CLSM image of the emulsions, (B) Visual appearance of the DCF-based oleogels, (C) PLM images of the DCF-based oleogels. The DCF concentrations of 2.5, 5.0, 7.5, 10.0 and 12.5% (w/v) in DCF-based oleogels were called OD2.5, OD5.0, OD7.5, OD10.0 and OD12.5, respectively.

the molecular chains of dietary fiber molecules are extended and orderly wound due to shear effects (Meng et al., 2018a). During water removal, the interaction between the dietary fiber molecules prevents the collapse of the network structure, resulting in a hybrid amorphous structure with semi-crystalline properties, which structures the oil. When the DCF concentration $>$ 7.5% (w/v), the peak intensity of the oleogels decreased, which may be due to the excessive winding of the dietary fiber chain, resulting in the formation of aggregates consistent with the observations of PLM (Xu et al., 2023).

3.1.3. ATR-FTIR analysis of oleogels

The ATR-FTIR spectra of DCF and oleogels are presented in Fig. 2B. The absorption peaks in each sample originate from the functional groups present in corn oil (**Fig. S2**) and DCF. The peak around 3300–3400 cm^{-1} corresponds to the stretching vibration of the -OH group, attributed to dietary fiber and protein in DCF. Broad peaks observed in the spectra of oleogels compared to DCF and corn oil indicate that the network structure primarily forms through tensile intramolecular or intermolecular hydrogen bonds between DCF and corn oil (Pan et al., 2021). The entanglement of hydrogen-bonded polymers promotes a relatively ordered structure of the oleogels, effectively trapping oil droplets within the network (Jiang et al., 2022). The peak at approximately 3010 cm^{-1} in the oleogels spectra corresponds to the = C-H stretching vibration in corn oil, while peaks at 2930 cm^{-1} and 2862 cm^{-1} correspond to the C—H stretching vibrations of CH in corn oil and DCF, respectively. The peak intensity in oleogels is lower than in DCF, likely due to van der Waals forces between alkyl groups in corn oil. The peak at 1743 cm^{-1} corresponds to the correlation of corn oil. Additionally, the 1556 cm^{-1} peak originates from the negatively charged carboxyl group (–COO–) of protein in DCF, which gradually weakens in the oleogels spectrum, indicating the presence of electrostatic interactions between corn oil and protein. There was no significant difference in the FTIR spectra of oleogels with different DCF concentrations. In summary, the main driving forces for forming DCF-based oleogels are hydrogen bonding, van der Waals forces, and electrostatic interactions.

3.1.4. OBC analysis of oleogels

The ability of the oleogels to immobilize oil was assessed by measuring OBC. Notably, OBC exhibited a substantial increase with increasing concentrations of DCF (Fig. 2C). Oleogels containing lower DCF levels demonstrated a moderate OBC ranging from 38.02% to 61.55%, indicating some oil separation under centrifugal force. However, for oleogels with DCF concentration exceeding 10.0% (w/v), the

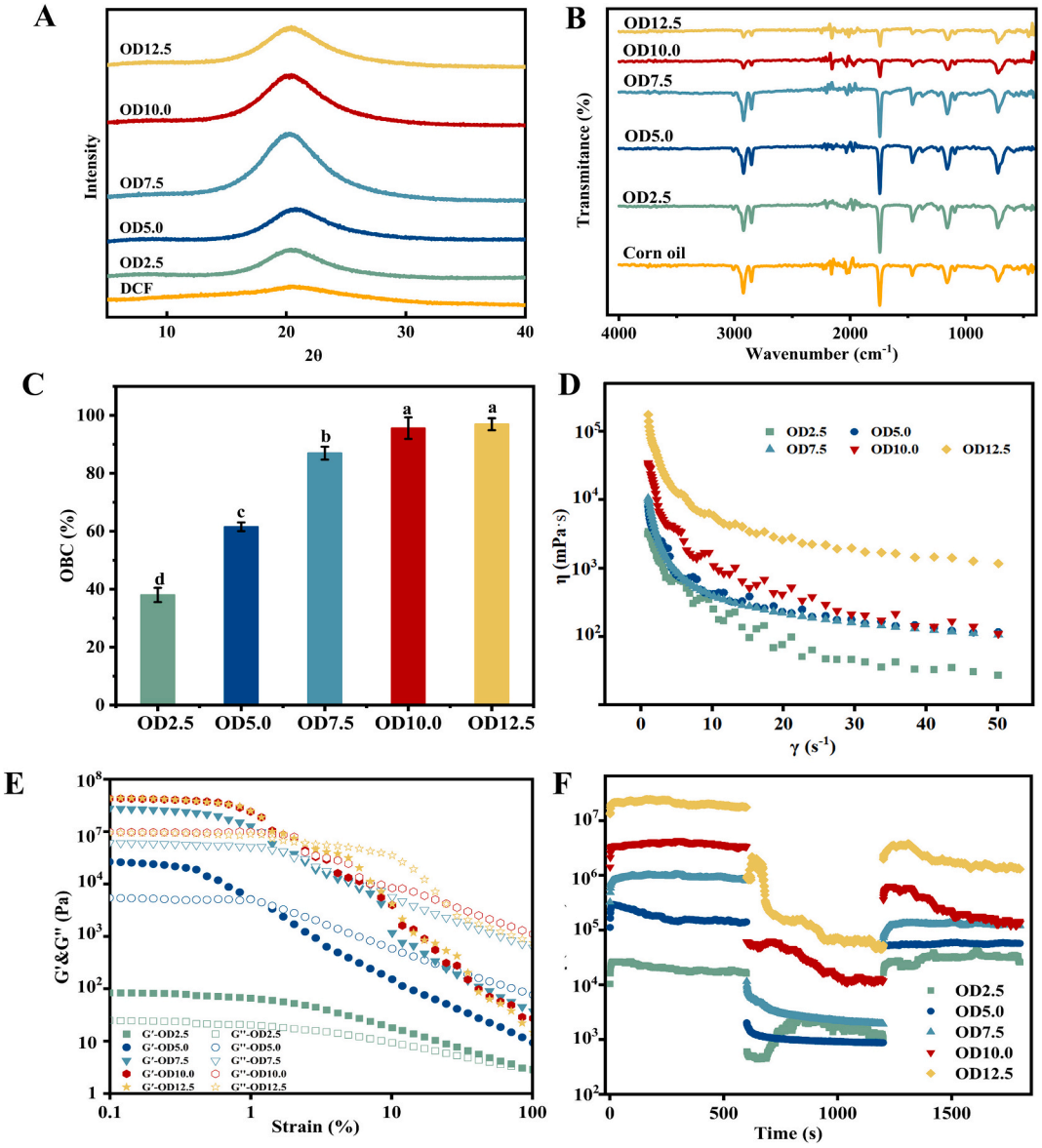

Fig. 2. Physical properties of DCF-based oleogels: (A) X-ray diffractograms, (B) ATR-FTIR spectra; (C) Oil binding capacity, (D) Apparent viscosity, (E) Three-interval thixotropy, (F) Amplitude sweep. The DCF concentrations of 2.5, 5.0, 7.5, 10.0 and 12.5% (w/v) in DCF-based oleogels were called OD2.5, OD5.0, OD7.5, OD10.0 and OD12.5, respectively. Samples with different letters indicate a significant difference ($p < 0.05$).

OBC surpassed 96.95%. The high OBC indicates that the network structure has developed sufficient integrity to retain nearly all of the oil, even under intense centrifugal stress (Meng et al., 2018b). This observation aligns with the microstructure of oleogels, where larger aggregates gradually formed.

3.1.5. Texture analysis of oleogels

In the TPA test, the oleogels were cyclically compressed twice to simulate property changes during chewing. Table 1 presents the results of different concentrations of DCF on the mechanical properties of the oleogels. Hardness, representing the maximum force received during the first compression cycle, also known as sample strength (Xie et al., 2023), increased as the DCF concentration rose from 5.0% to 10.0% (w/v). This increase can be attributed to the greater number of molecules forming the oleogels network, leading to a tighter network structure and gel structure positively correlated with DCF concentration. Chewiness, defined as the amount of energy required to chew solid food until it is ready to swallow, exhibited a trend similar to hardness. Chen et al. (2023) also reported a similar effect of polymer concentration on the texture properties of oleogels.

Table 1
The hardness, springiness, cohesiveness, and chewiness of the DCF-based oleogels.

DCF(%)	Hardness (N)	Cohesiveness	Springiness (mm)	Chewiness(g)
2.5	-	-	-	-
5.0	0.65 ± 0.07^{c}	0.66 ± 0.03^{a}	9.90 ± 0.10^{a}	3.94 ± 0.73^{c}
7.5	1.43 ± 0.14^{b}	0.37 ± 0.06^{b}	10.00 ± 0.02^{a}	4.63 ± 0.11^{bc}
10.0	2.07 ± 0.07^{b}	0.24 ± 0.02^{c}	9.95 ± 0.03^{a}	5.43 ± 0.52^{b}
12.5	3.97 ± 0.42^{a}	0.14 ± 0.02^{d}	9.19 ± 0.60^{b}	6.40 ± 0.04^{a}

Note: Different letters mean the significance ($p < 0.05$). "-" represents that the oleogels has fluidity and cannot accurately determine the texture.

3.1.6. Rheological properties analysis of oleogels

Characterize the rheological behavior of oleogels, including frequency sweeps, viscosity, oscillatory stress sweeps, and flow properties, to obtain more information on the effect of DCF concentration on the

structural properties of oleogels (Fig. 2S). It shows that G' is consistently greater than G" during the frequency scan, indicating a gel-like rheological behavior of the oleogels. Additionally, as the frequency increases, G′ exhibits a slight increase, implying that the oleogels are frequency-dependent and possess a strong gel signature characteristic of a non-covalent "physical" cross-linking network (Xie et al., 2023).

As shown in Fig. 2D, the oleogels display shear-thinning behavior. The DCF concentration significantly influences the apparent viscosity of oleogels. At the same shear frequency, the apparent viscosity of oleogels increases with higher DCF concentrations. Stronger interaction between dietary fiber in higher concentrations of DCF results in enhanced gel strength and shear resistance of the oil crystal network structure (Xu et al., 2023).

All samples exhibited solid characteristics (G′ > G″) under shear stress testing (Fig. 2E). Due to the slight phase separation, the oleogels prepared with 2.5% (w/v) DCF had a loose structure, resulting in a lower G'. Higher DCF concentrations led to a more structured oleogels with higher G' and yield strain values, indicating stronger network structure (Pan et al., 2021). In addition, the intersection of G′ and G″ was observed in the stress range of 0.1–100% and increased with the DCF concentration, indicating that the oleogels structure became increasingly stable under external forces (Espert et al., 2021). Compared to tamarind seed polysaccharide-gelatin constructed oleogels, DCF-based oleogels exhibited higher gel strength (G′) and yield strain (Xie et al., 2023).

The three-interval thixotropy test (Fig. 2F) revealed that at a constant shear rate, the viscosity of the oleogels samples decreased slowly over time. As the shear rate sharply increased from 0.1 s^{-1} to 10 s^{-1}, the viscosity of the oleogels decreased significantly, likely due to the disruption of weak hydrogen bonding within the oleogels. Conversely, when the shear rate decreases sharply from 10 s^{-1} to 0.1 s^{-1}, the viscosity of the oleogels immediately recovers. This recovery is attributed to the reformation of hydrogen bond interactions and the restoration of the sample structure following the removal of external force (Meng et al., 2018b). The structural recovery of the oleogels increases and then decreases with increasing DCF concentration. This phenomenon may be linked to aggregates within the oleogels network structures at DCF concentrations >10.0% (w/v), hindering the recombination of hydrogen bonds. In conclusion, owing to their excellent rheological and mechanical properties, oleogels exhibit potential applications in food processing.

3.2. Surimi gel properties

3.2.1. TPA and gel strength of surimi

TPA analysis simulates oral chewing movements in humans to evaluate the sensory properties of surimi gel. Fig. 3A-D illustrates the quality of surimi prepared from corn oil and oleogels with varying concentrations of DCF. Previous studies have indicated that adding oil to surimi gel can influence its texture properties through protein-oil interactions (Yu et al., 2022). Compared to the control group, the CO group reduced the textural properties (hardness, springiness, cohesiveness, and chewiness) of the surimi gel. The incorporation of corn oil hindered the unfolding and rearrangement of surimi protein, leading to reduced hydrogen bonding and hydrophobic interactions between protein, resulting in a looser structure of the surimi gel and decreased texture (Zhang, Xie, et al., 2023). The oleogels group effectively mitigated this negative effect ($p < 0.05$). Hardness, springiness, cohesiveness and chewiness of oleogels groups were significantly higher than corn oil group. Oleogels acted as active fillers in the surimi gel, increasing hydrophobic interactions to promote a more uniform and dense gel structure, thereby improving the texture properties of the surimi gel (Zhang, Lu, et al., 2023). The hardness, cohesiveness, and chewiness of surimi in the OD5.0 group were comparable to those in the control group. The decrease in texture characteristics of surimi in the OD2.5 oleogels group may be related to its lower oil-holding capacity. OD2.5 contains a large amount of liquid oil, and the oil droplets hinder the interaction of surimi protein. The decrease in surimi textural characteristics in oleogels with higher DCF concentration may be related to the texture of the oleogels. The rough and rugged texture of oleogels may increase the gaps between surimi gels, interfere with surimi protein

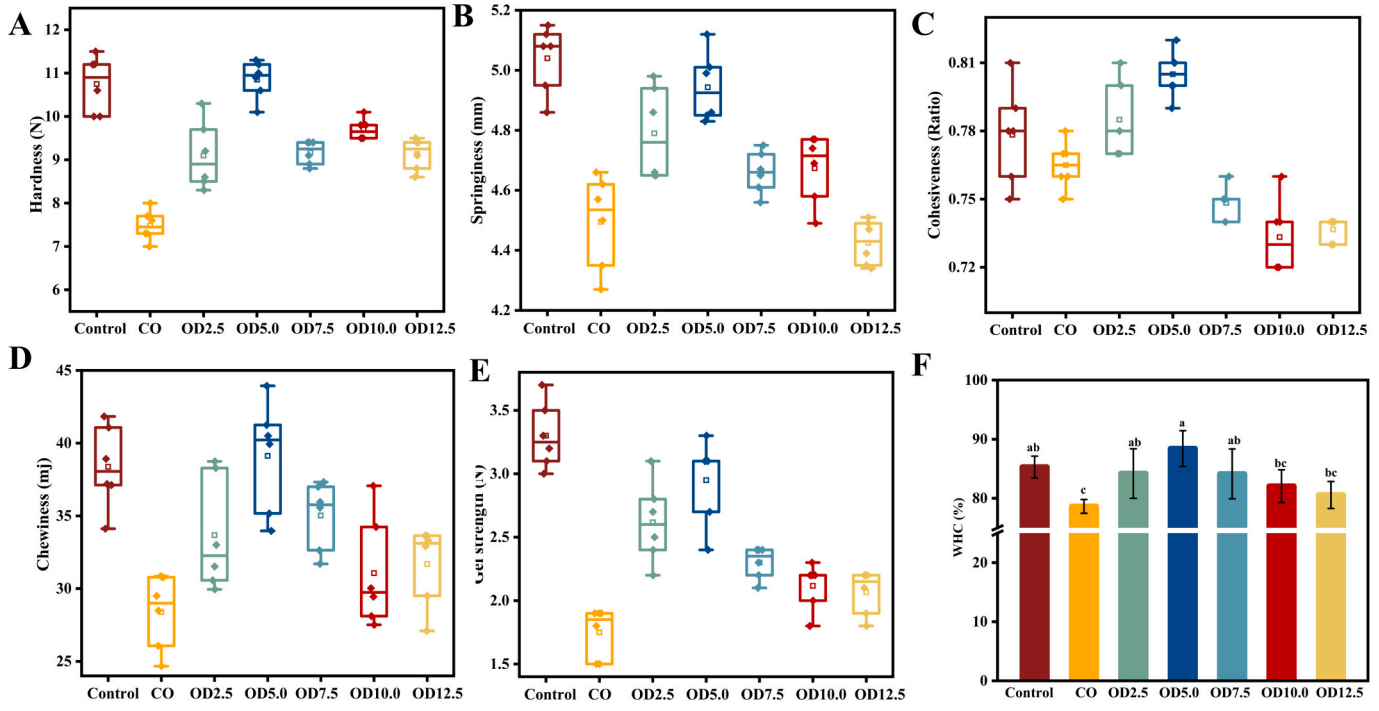

Fig. 3. Effect of different treatments on the texture profile (A-D, represents hardness, springiness, cohesiveness, chewiness), gel strength (E), and water holding capacity (F) of surimi. The box represents the 25%–75% confidence interval of the data and the horizontal line represents the mean. The DCF concentrations of 2.5, 5.0, 7.5, 10.0 and 12.5% (w/v) in DCF-based oleogels were called OD2.5, OD5.0, OD7.5, OD10.0 and OD12.5, respectively. The surimi gel with corn oil group was named "CO". Different lower letters indicate significant differences between the different treatment groups ($p < 0.05$).

interactions, and destroy the gel network structure.

Gel strength is a crucial indicator of surimi product quality, directly impacting its commercial value (Zhang, Lu, et al., 2023). The gel strength results (Fig. 3E) indicate that the oleogels group significantly enhanced the gel strength of surimi compared to the CO group ($p < 0.05$). The impact of oleogels on the gel strength of surimi increased initially and then decreased with the rise in DCF concentration. The gel strength of the OD5.0 group reached its peak, aligning with the TPA findings. Lu et al. (2022) found that a reduction in hydrophobic interactions might decrease in gel strength. The surimi gel results further illustrate that oleogels with higher concentrations of DCF hinder the binding of non-covalent bonds between surimi protein.

3.2.2. WHC of surimi

The WHC of surimi reflects the gel network's ability to retain water molecules under external forces. As shown from Fig. 3F, the oleogels group significantly augmented the WHC of surimi compared to the CO group. When the DCF concentration ranged from 2.5% to 5.0% (w/v), the oleogels notably increased the WHC of the surimi gel. However, with DCF concentrations exceeding 7.5% (w/v), the WHC of the surimi gel decreased. This phenomenon may be attributed to: 1) The pore-filling effect of DCF-based oleogels, which enhances their water-binding capacity by reducing fluidity (Lv et al., 2023); 2) During surimi production, DCF-based oleogels might undergo re-emulsification, constraining water mobility and fostering hydrophobic interactions among surimi

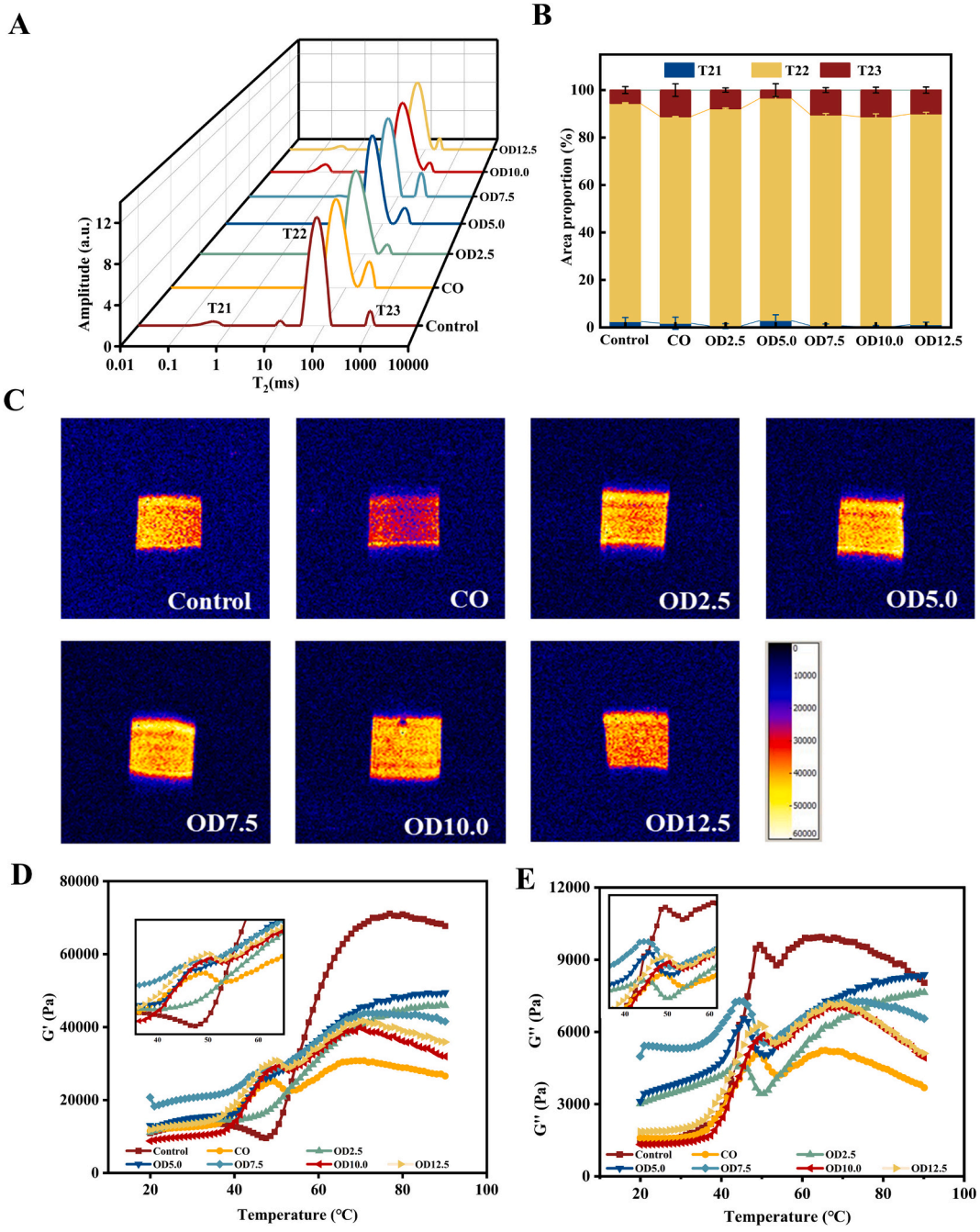

Fig. 4. The curves of relaxation time (A), peak areas proportion (B) and hydrogen proton weighted image (C) of surimi under different treatments. Changes in G′ (D) and G‟ (E) of surimi with temperature sweep. The DCF concentrations of 2.5, 5.0, 7.5, 10.0 and 12.5% (w/v) in DCF-based oleogels were called OD2.5, OD5.0, OD7.5, OD10.0 and OD12.5, respectively. The surimi gel with corn oil group was named "CO". Different lower letters indicate significant differences between the different treatment groups ($p < 0.05$).

protein (Chen & Yang, 2019).

3.2.3. Water distribution of surimi

The distribution of water molecules in oil-fortified surimi were assessed using LF-NMR, providing insights into water and oil distribution within the gel. The T2 relaxation time curves exhibited 2–3 significant peaks. T21 (0.1–10 ms) represents water tightly bound to various protein macromolecules, T22 (10–100 ms) corresponds to immobile water within the three-dimensional network structure, and T23 (100–1000 ms) indicates the presence of free water (Lu et al., 2022; Ye et al., 2022). The inversion curve and content changes are presented in Fig. 4A-B. Compared to the control group, the CO group showed a decrease in the proportion of the T22 area and an increase in the proportion of the T23 area in the surimi, indicating a significant loss of immobile water due to the presence of corn oil. Corn oil may act as an inactive filler, weakening the gel network of surimi. In contrast, oleogels effectively addressed this drawback. With increasing DCF concentration in oleogels, the proportion of T22 and T23 areas in the surimi gel initially increased and then decreased. The OD5.0 group exhibited the highest proportion of T22 area and the lowest proportion of T23 area in the surimi gel, comparable to the control group. Oleogels with 5.0% (w/v) DCF can efficiently convert the free water in the surimi gel into fixed water, which may be achieved by forming a dense gel network with surimi protein by hydrophobic interactions (Liu et al., 2023), consistent with WHC results.

Observing the water distribution in the surimi gel with and without oil using MRI (Fig. 4C). The color intensity in the NMR image reflects the density of hydrogen protons distributed in the surimi gel, where yellow indicates high proton density, and blue indicates low proton density. The CO group exhibited more dark red spots than the control group, indicating uneven water distribution and a low water retention rate. However, the surimi supplemented with oleogels showed relatively fewer dark red spots, suggesting that oleogels had fewer adverse effects on the water distribution of surimi. The density of hydrogen proton distribution was the highest in the OD5.0 group. Furthermore, the density of hydrogen protons in the surimi in the oleogels group with DCF concentrations of 7.5–12.5% (w/v) decreased. After adding the oleogels with 5.0% (w/v) DCF, the network structure of the surimi gel was denser and more water was captured. These results further confirm our LF-NMR findings and changes in WHC.

3.2.4. Rheological properties of surimi

In order to study the gelatinization characteristics of surimi, the heat-induced gelation process of surimi prepared from oleogels was studied using the dynamic rheological method. The viscoelasticity of the protein network formed in the surimi is denoted by G', while G" denotes the viscosity of the surimi (Roy et al., 2021). As shown in Fig. 4D, at the initial stage of heating (20–40 °C), the G' value of surimi in the oleogels group was higher than that in the control group and the CO group. Oleogels may have strengthened the weak gel structure of surimi formation. In the middle of heating (40–59 °C), the G' value of the control group decreased rapidly with the gradual temperature increase, reaching the lowest at 55 °C. The G' value decreased may be related to the cleavage of hydrogen bonds and the aggregation of surimi protein. In contrast, G' increased in the CO and oleogels groups, suggesting that the aggregation pattern of surimi protein changed due to the adding oil, with most of the surimi protein being encapsulated by corn oil and oleogels, affecting the denaturation temperature (Zhang et al., 2021). In the late heating phase (55–90 °C), as the temperature increased, the cross-linking between undegraded and structurally intact protein molecules promoted the formation of a more stable surimi gel network (Fang et al., 2021). The G' of surimi in the control group increased rapidly, while the G' of the CO and oleogels groups increased slowly. Corn oil and oleogels hindered the unfolding of surimi protein molecules and interfered with the hydrophobic interactions between proteins. However, the G' of surimi in the oleogels group was higher than that in the CO group, and it first increased and then decreased with the increase of DCF concentration. These results demonstrate that the surimi gel formed by the oleogels group had better viscoelasticity than the CO group and had better gel elasticity. The G" value was significantly lower than the G' value over the entire test temperature range (Fig. 4E), showing a consistent trend with the G' value, indicating that the elastomeric gel is the main feature of surimi gel. At 90 °C, the G' and G" values of the surimi gels in the OD5.0 group were the highest, indicating the highest viscoelasticity. The reduction of G' and G" in the oleogels group with high concentrations of DCF can be attributed to its high stiffness, resulting in flocculation in surimi gel, affecting cross-linking between surimi proteins.

3.2.5. Micromorphology of surimi

In Fig. 5A, the red area represents the stained oil droplet or emulsion droplet in the surimi gel, while the irregular white area indicates the gel cavity. It was observed that the control group had very few red spots, but when corn oil or oleogels were added, the number of red spots increased dramatically, accompanied by the appearance of more irregular white areas. In the CO group, larger voids appeared, indicating that the oil droplets were accumulating, resulting in an irregular gel network structure. However, no significant red spots were observed, possibly due to weaker oil-protein interactions, leading to the oil being washed off during the staining process with ORO dye (60% isopropanol). Yan et al. (2020) reported that high levels of fish oil led to lipid aggregation, hindering protein cross-linking and resulting in a looser network structure. In contrast, the OD5.0 group exhibited an increasingly compact structure with smaller, more homogeneous oil droplets, indicating that the oleogels with 5.0% (w/v) DCF could be uniformly dispersed in the surimi gel. Furthermore, the strong interaction between oleogels and surimi protein led to a tight gel network structure. The OD2.5 group exhibited a loose structure, possibly due to its low oil-holding capacity and gel strength. On the other hand, the OD7.5, OD10.0, and OD12.5 groups had larger voids and larger droplets, possibly due to the stronger gel network structure of the oleogels, which formed larger aggregates with surimi protein, thereby weakening the formation of the surimi gel network.

In Fig. 5B, SEM provides a closer look at the microstructure of the surimi gel in the presence of oleogels. The CO group exhibited large voids within the surimi gel, indicating an irregular and porous structure. In contrast, the microstructure of the oleogels group appeared more uniform and denser. This difference can be attributed to the oleogels acting as an active filler within the surimi gel. The oleogels promoted the compact and smooth structure of the surimi gel. The best effect of surimi gel in the OD5.0 group showed that the oleogels with 5.0% (w/v) DCF formed a stronger protein-lipid interaction with surimi protein. Furthermore, the DCF present in the oleogels likely contributes to the formation of the surimi gel network. Roy et al. (2021) pointed out that emulsifiers can influence the content of myosin in meat, which in turn affects protein gelation. Adding oleogels, especially those with optimal DCF concentrations, can affect the gelatinization properties of surimi, resulting in a more desirable microstructure.

3.2.6. Changes in chemical forces in surimi

Chemical forces such as ionic, hydrogen, and hydrophobic bonds maintain the gel network structure of surimi gels (Tan et al., 2024). As shown in Fig. 5C, hydrophobic interactions emerge as the predominant force shaping the surimi gel network structure. Yu et al. (2022) previously noted that oil can modulate hydrophobic interactions by influencing protein-protein interactions and altering the protein environment within surimi gels. The CO group exhibited the lowest level of hydrophobic interactions, likely due to the binding of corn oil to surimi protein, which weakened protein-protein interactions. In contrast, the oleogels group displayed an increase and subsequent decrease in hydrophobic interaction with DCF concentration, with the OD5.0 group exhibiting the highest hydrophobic force content. This increase in

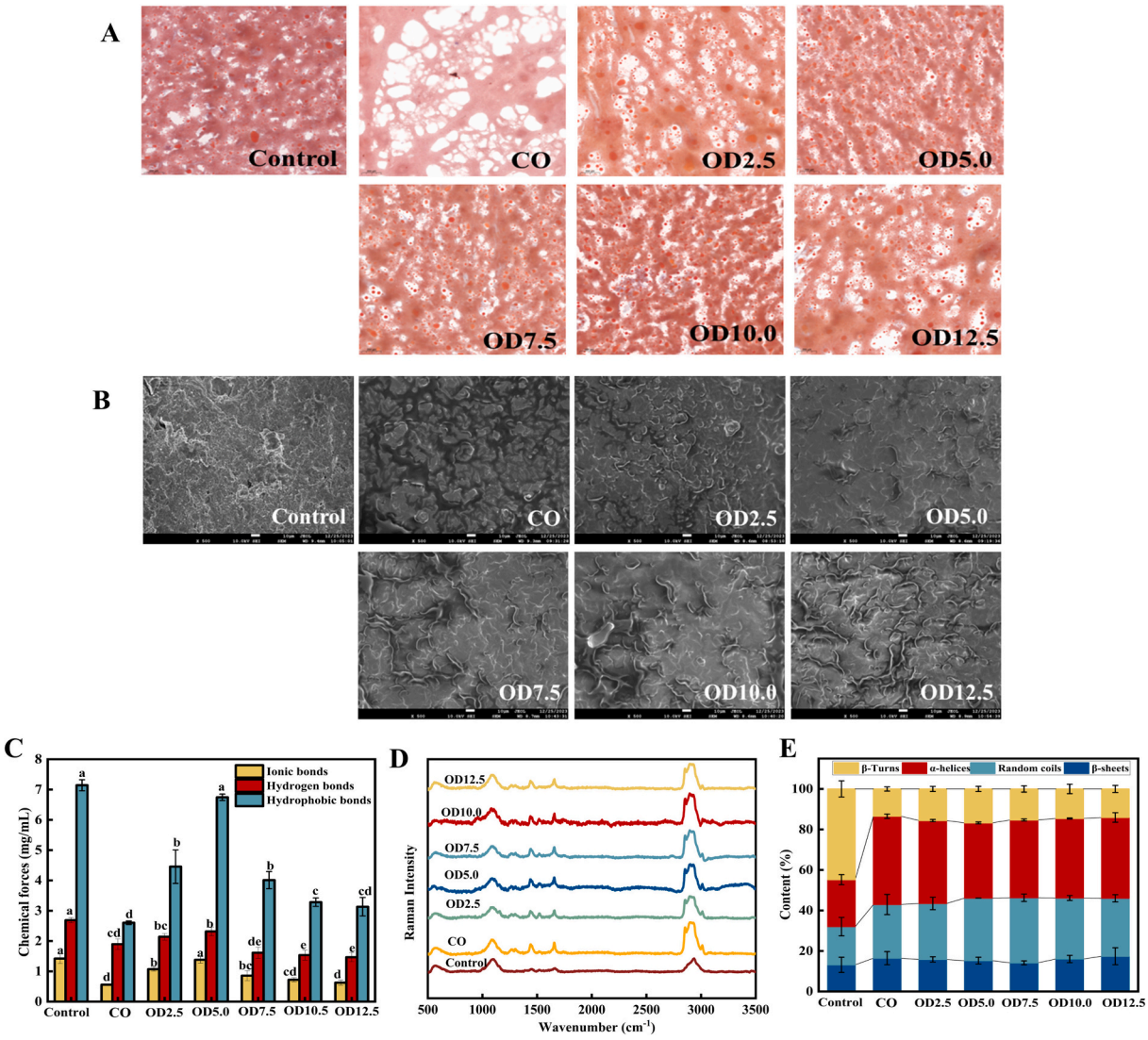

Fig. 5. Oil red O (ORO) (A) and Scanning electron microscopy (SEM) (B) micrographs and chemical forces (C) in surimi under different treatments; Raman spectroscopy (D) of surimi from different treatment groups. The changes in protein secondary structure (α-helix, β-sheet, β-turn and random coil) (E) in surimi under different treatments. The DCF concentrations of 2.5, 5.0, 7.5, 10.0 and 12.5% (w/v) in DCF-based oleogels were called OD2.5, OD5.0, OD7.5, OD10.0 and OD12.5, respectively. The surimi gel with corn oil group was named "CO". Different lower letters indicate significant differences between the different treatment groups ($p < 0.05$). (For interpretation of the references to color in this figure legend, the reader is referred to the web version of this article.)

hydrophobic force can be attributed to the structural role of oleogels structured corn oil, effectively reducing oil-protein binding and enhancing protein cross-linking (Liu et al., 2023). However, the high viscosity of oleogels with high DCF concentrations hindered the uniformly dispersion of the surimi gel network, resulted in larger cavities in the gel network and negatively affecting protein-protein interactions. Ionic bonds is electrostatic interactions between oppositely charged amino acid residues. Oleogels groups enhance the electrostatic interaction between proteins. During the heating of surimi, oleogels groups may lead to partial denaturation of the protein molecules, exposing more positively and negatively charged amino acid residues, thus altering the charge distribution of the proteins (Zhou et al., 2017). The trend of hydrogen and ionic bonds is consistent with hydrophobic interactions.

3.2.7. *Changes in the secondary structure in surimi*

In Fig. 5E, Raman spectroscopy reveals changes in the protein secondary structure of surimi, particularly focusing on the amide I bands within the range of 1600–1700 cm^{-1}, indicative of various structural elements (Kobayashi et al., 2017). Correspondingly, Fig. 5G provides a quantitative analysis of protein secondary structure based on amide I spectroscopy. Compared to the control group, the CO group exhibited a significant increase in α-helix content, accompanied by a decrease in β-fold and β-turn contents ($p < 0.05$). This shift is attributed to the hydrophobic side chains of surimi proteins binding to oil droplets, promoting denaturation and the stretching of hydrogen bonds. It is noteworthy that α helix tends to weaken protein gelation, whereas β-fold or random coil structure favor the formation of denser gel networks (Yan et al., 2020). However, the detrimental effects observed in the CO group were effectively mitigated by the oleogels group. At DCF concentrations of 2.5–5.0% (w/v), the oleogels group showed a decrease in α-helix content and an increase in β-turn and random helix content. Oleogels with lower concentrations of DCF might promote the transformation of protein α-helix to other secondary structures. Conversely, at DCF concentrations >5.0% (w/v), the oleogels group exhibited an increase in α-helix content and a decrease in β-turn and random helix content. Oleogels with higher DCF concentrations hindered the formation of dense surimi gel networks, potentially due to the weakening of hydrogen bonding between protein induced by high DCF concentrations.

4. Conclusions

This study investigated the preparation of DCF-based oleogels and its application in oil-fortified surimi gel. These oleogels exhibited soft solids characteristics, favorable viscoelasticity, and oil binding capacity. Microstructural analysis, along with FTIR and XRD results, confirmed that the entanglement and chain extension between dietary fiber played pivotal roles in forming the three-dimensional network structure of DCF-based oleogels. Specifically, hydrogen bonding emerged as the primary driving force behind forming this network structure, as indicated by FTIR findings. Furthermore, the impact of DCF-based oleogels in preparing oil-fortified surimi was thoroughly explored. It was observed that these oleogels significantly alleviated the adverse effects typically associated with the addition of corn oil, particularly on the gel strength, WHC, and texture of surimi. Notably, the surimi prepared with oleogels containing 5.0% (w/v) DCF exhibited gel strength comparable to that of the control group. Meanwhile, Oleogels enhanced the gel properties of surimi through hydrophobic interactions and alterations in the secondary structure of surimi protein. This study provides a valuable theoretical basis and practical guidance for developing oil-fortified surimi gel products using DCF-based oleogels.

CRediT authorship contribution statement

Xia Gao: Data curation, Investigation, Writing – original draft. **Zhisheng Pei:** Writing – review & editing. **Xiangzhou Yi:** Writing – review & editing. **Xuan Zhang:** Formal analysis. **Dongxue He:** Methodology. **Zilan Feng:** Validation. **Guanghua Xia:** Funding acquisition. **Xuanri Shen:** Funding acquisition.

Declaration of competing interest

No conflicts of interest are declared for any of the authors.

Data availability

No data was used for the research described in the article.

Acknowledgments

This research was funded by the Key R&D Plan of Hainan Province (NO. ZDYF2021XDNY284), Scientific Research Foundation of Hainan Tropical Ocean University (RHDRC202314), and the Key R&D Plan of Hainan Province (NO. ZDYF2022XDNY335).

Appendix A. Supplementary data

Supplementary data to this article can be found online at https://doi.org/10.1016/j.fochx.2024.101635.

References

Bao, P. Q., Chen, L., Hu, Y., Wang, Y., & Zhou, C. L. (2022). L-arginine and L-lysine retard aggregation and polar residue modifications of myofibrillar proteins: Their roles in solubility of myofibrillar proteins in frozen porcine. *Food Chemistry, 393*, Article 133347. https://doi.org/10.1016/j.foodchem.2022

Chen, X. W., & Yang, X. Q. (2019). Characterization of orange oil powders and oleogels fabricated from emulsion templates stabilized solely by a natural triterpene saponin. *Journal of Agricultural and Food Chemistry, 67*(9), 2637–2646. https://doi.org/10.1021/acs.jafc.8b04588

Chen, X. W., Zhang, H., Li, X. X., & Sun, S. D. (2023). Edible HIPE-gels and oleogels formed by synergistically combining natural triterpenoid saponin and citrus dietary fiber. *Carbohydrate Polymers, 305*, Article 120499. https://doi.org/10.1016/j.carbpol.2022.120499

Espert, M., Hernández, M. J., Sanz, T., & Salvador, A. (2021). Reduction of saturated fat in chocolate by using sunflower oil-hydroxypropyl methylcellulose based oleogels. *Food Hydrocolloids, 120*, Article 106917. https://doi.org/10.1016/j.foodhyd.2021

Fang, Q., Shi, L. F., Ren, Z. Y., Hao, G. X., Chen, J., & Weng, W. Y. (2021). Effects of emulsified lard and TGase on gel properties of threadfin bream *(Nemipterus virgatus)* surimi. *LWT- Food Science and Technology, 146*, Article 111513. https://doi.org/10.1016/j.lwt.2021

He, D., Yi, X. Z., Xia, G. H., Liu, Z. Y., Zhang, X. Y., Li, C., & Shen, X. R. (2022). Effects of fish oil on the gel properties and emulsifying stability of myofibrillar proteins: A comparative study of tilapia, hairtail and squid. *LWT- Food Science and Technology, 161*, Article 113373. https://doi.org/10.1016/j.lwt.2022

Jiang, Q., Li, P., Ji, M., Du, L., Li, S., Liu, Y., & Meng, Z. (2022). Synergetic effects of water-soluble polysaccharides for intensifying performances of oleogels fabricated by oil-absorbing cryogels. *Food Chemistry, 372*, Article 131357. https://doi.org/10.1016/j.foodchem.2021.131357

Keshanidokht, S., Kumar, S., Thulstrup, P. W., Via, M. A., Clausen, M. P., & Risbo, J. (2023). Thermo-responsive behavior of glycerol-plasticized oleogels stabilized by zein. *Food Hydrocolloids, 139*, Article 108582. https://doi.org/10.1016/j.foodhyd.2023

Kobayashi, Y., Mayer, S. G., & Park, J. W. (2017). FT-IR and Raman spectroscopies determine structural changes of tilapia fish protein isolate and surimi under different comminution conditions. *Food Chemistry, 226*, 156–164. https://doi.org/10.1016/j.foodchem.2017.01.068

Li, L., Liu, G., Bogojevic, O., Pedersen, J. N., & Guo, Z. (2022). Edible oleogels as solid fat alternatives: Composition and oleogelation mechanism implications. *Comprehensive Reviews in Food Science and Food Safety, 21*(3), 2077–2104. https://doi.org/10.1111/1541-4337.12928

Li, X., Guo, G., Zou, Y., Luo, J., Sheng, J., Tian, Y., & Li, J. (2023). Development and characterization of walnut oleogels structured by cellulose nanofiber. *Food Hydrocolloids, 142*, Article 108849. https://doi.org/10.1016/j.foodhyd.2023.108849

Liao, H., Jiang, T., Chen, L., Wang, G., Shen, Q., Liu, X., Ding, W., & Zhu, L. (2024). Stability and 3D-printing performance of high-internal-phase emulsions based on ultrafine soybean meal particles. *Food Chemistry, 449*, Article 139172. https://doi.org/10.1016/j.foodchem.2024.139172

Liu, Y., Huang, Y., Wang, Y., Zhong, J., Li, S., Zhu, B., & Dong, X. (2023). Application of cod protein-stabilized and casein-stabilized high internal phase emulsions as novel fat substitutes in fish cake. *LWT- Food Science and Technology, 173*, Article 114267. https://doi.org/10.1016/j.lwt.2022

Lu, Y., Zhu, Y., Ye, T., Nie, Y., Jiang, S., Lin, L., & Lu, J. (2022). Physicochemical properties and microstructure of composite surimi gels: The effects of ultrasonic treatment and olive oil concentration. *Ultrasonics Sonochemistry, 88*, Article 106065. https://doi.org/10.1016/j.ultsonch.2022

Lv, Y., Sun, X., Jia, H., Hao, R., Jan, M., Xu, X., Li, S., Dong, X., & Pan, J. (2023). Antarctic krill (*Euphausia superba*) oil high internal phase emulsions improved the lipid quality and gel properties of surimi gel. *Food Chemistry, 423*, Article 136352. https://doi.org/10.1016/j.foodchem.2023

Meng, Z., Qi, K. Y., Guo, Y., Wang, Y., & Liu, Y. F. (2018a). Effects of thickening agents on the formation and properties of edible oleogels based on hydroxypropyl methyl cellulose. *Food Chemistry, 246*, 137–149. https://doi.org/10.1016/j.foodchem.2017.10.154

Meng, Z., Qi, K. Y., Guo, Y., Wang, Y., & Liu, Y. F. (2018b). Macro-micro structure characterization and molecular properties of emulsion-templated polysaccharide oleogels. *Food Hydrocolloids, 77*, 17–29. https://doi.org/10.1016/j.foodhyd.2017.09.006

Pan, H. B., Xu, X. L., Qian, Z. Q., Cheng, H., Shen, X. M., Chen, S. G., & Ye, X. Q. (2021). Xanthan gum-assisted fabrication of stable emulsion-based oleogel structured with gelatin and proanthocyanidins. *Food Hydrocolloids, 115*, Article 106596. https://doi.org/10.1016/j.foodhyd.2021

Pei, Z., Wang, H., Xia, G., Hu, Y., Xue, C., Lu, S., Li, C., & Shen, X. (2023). Emulsion gel stabilized by tilapia myofibrillar protein: Application in lipid-enhanced surimi preparation. *Food Chemistry, 403*, Article 134424. https://doi.org/10.1016/j.foodchem.2022.134424

Rodsamran, P., & Sothornvit, R. (2018). Physicochemical and functional properties of protein concentrate from by-product of coconut processing. *Food Chemistry, 241*, 364–371. https://doi.org/10.1016/j.foodchem.2017.08.116

Roy, V. C., Chamika, W. A. S., Park, J. S., Truc, C. H., Khan, F., Kim, Y. M., & Chun, B. S. (2021). Preparation of bio-functional surimi gel incorporation of fish oil and green tea extracts: Physico-chemical activities, in-vitro digestibility, and bacteriostatic properties. *Food Control, 130*, Article 108402. https://doi.org/10.1016/j.foodcont.2021.108402

Sharma, R., Yadav, S., Yadav, V., Akhtar, J., Katari, O., Kuche, K., & Jain, S. (2023). Recent advances in lipid-based long-acting injectable depot formulations. *Advanced Drug Delivery Reviews, 199*, Article 114901. https://doi.org/10.1016/j.addr.2023.114901

Shi, L., Wang, X. F., Chang, T., Wang, C. J., Yang, H., & Cui, M. (2014). Effects of vegetable oils on gel properties of surimi gels. *LWT- Food Science and Technology, 57*(2), 586–593. https://doi.org/10.1016/j.lwt.2014.02.003

Su, Y. J., Zhang, W. Q., Liu, R. D., Chang, C. H., Li, J. H., Xiong, W., … Gu, L. P. (2023). Emulsion-templated liquid oil structuring with egg white protein microgel - xanthan gum. *Foods, 12*(9), 1884. https://doi.org/10.3390/foods12091884

Tan, Y., Li, S., Liu, S., & Li, C. (2023). Modification of coconut residue fiber and its bile salt adsorption mechanism: Action mode of insoluble dietary fibers probed by microrheology. *Food Hydrocolloids, 136*, Article 108221. https://doi.org/10.1016/j.foodhyd.2022.108221

Tan, Z., Yang, X., Wang, Z., Chen, Z., Pan, J., Sun, Q., & Dong, X. (2024). Konjac glucomannan-assisted fabrication of stable emulsion-based oleogels constructed with pea protein isolate and its application in surimi gels. *Food Chemistry, 443*, Article 138538. https://doi.org/10.1016/j.foodchem.2024.138538

Tavernier, I., Patel, A. R., Van der Meeren, P., & Dewettinck, K. (2017). Emulsion-templated liquid oil structuring with soy protein and soy protein: κ-carrageenan

complexes. *Food Hydrocolloids, 65*, 107–120. https://doi.org/10.1016/j.foodhyd.2016.11.008

Trinidad, T. P., Mallillin, A. C., Valdez, D. H., Loyola, A. S., Askali-Mercado, F. C., Castillo, J. C., … Chua, M. T. (2006). Dietary fiber from coconut flour: A functional food. *Innovative Food Science & Emerging Technologies, 7*(4), 309–317. https://doi.org/10.1016/j.ifset.2004.04.003

Vélez-Erazo, E. M., Okuro, P. K., Gallegos-Soto, A., da Cunha, R. L., & Hubinger, M. D. (2022). Protein-based strategies for fat replacement: Approaching different protein colloidal types, structured systems and food applications. *Food Research International, 156*, Article 111346. https://doi.org/10.1016/j.foodres.2022.111346

Xie, F., Ren, X. L., Zhu, Z. J., Luo, J. Y., Zhang, H., Xiong, Z. Q., … Ai, L. Z. (2023). Tamarind seed polysaccharide-assisted fabrication of stable emulsion-based oleogel structured with gelatin: Preparation, interaction, characterization, and application. *Food Hydrocolloids, 142*, Article 108761. https://doi.org/10.1016/j.foodhyd.2023.108761

Xu, Y. Y., Sun, H., Lv, J., Wang, Y. W., Zhang, Y., & Wang, F. J. (2023). Effects of polysaccharide thickening agent on the preparation of walnut oil oleogels based on methylcellulose: Characterization and delivery of curcumin. *International Journal of Biological Macromolecules, 232*, Article 123291. https://doi.org/10.1016/j.ijbiomac.2023.123291

Yan, B. W., Jiao, X. D., Zhu, H. P., Wang, Q., Huang, J. L., Zhao, J. X., … Fan, D. M. (2020). Chemical interactions involved in microwave heat-induced surimi gel fortified with fish oil and its formation mechanism. *Food Hydrocolloids, 105*, Article 105779. https://doi.org/10.1016/j.foodhyd.2020.105779

Ye, Y. H., Liu, X. Y., Bai, W. D., Zhao, W. H., Zhang, Y., Dong, H., & Pan, Z. H. (2022). Effect of microwave-ultrasonic combination treatment on heating-induced gel properties of low-sodium tilapia surimi during gel setting stage and comparative analysis. *LWT- Food Science and Technology, 161*, Article 113386. https://doi.org/10.1016/j.lwt.2022.113386

Yi, X. Z., Pei, Z. S., Xia, G. H., Liu, Z. Y., Shi, H. H., & Shen, X. R. (2023). Interaction between liposome and myofibrillar protein in surimi: Effect on gel structure and digestive characteristics. *International Journal of Biological Macromolecules, 253*, Article 126731. https://doi.org/10.1016/j.ijbiomac.2023.126731

Yu, J., Song, L., Xiao, H., Xue, Y., & Xue, C. (2022). Structuring emulsion gels with peanut protein isolate and fish oil and analyzing the mechanical and microstructural characteristics of surimi gel. *LWT- Food Science and Technology, 154*, Article 112555. https://doi.org/10.1016/j.lwt.2021.112555

Zhang, C., Lu, M. X., Ai, C., Cao, H., Xiao, J. B., Imran, M., … Teng, H. (2023). Ultrasonic treatment combined with curdlan improves the gelation properties of low-salt *Nemipterus virgatus* surimi. *International Journal of Biological Macromolecules, 248*, Article 125899. https://doi.org/10.1016/j.ijbiomac.2023.125899

Zhang, R. F., Zhang, T., Hu, M. Y., Xue, Y., & Xue, C. H. (2021). Effects of oleogels prepared with fish oil and beeswax on the gelation behaviors of protein recovered from Alaska Pollock. *LWT- Food Science and Technology, 137*, Article 110423. https://doi.org/10.1016/j.lwt.2020.110423

Zhang, X., Xie, W., Liang, Q., Jiang, X., Zhang, Z., & Shi, W. (2023). High inner phase emulsion of fish oil stabilized with rutin-grass carp (*Ctenopharyngodon idella*) myofibrillar protein: Application as a fat substitute in surimi gel. *Food Hydrocolloids, 145*, Article 109115. https://doi.org/10.1016/j.foodhyd.2023.109115

Zheng, H., Mao, L., Cui, M., Liu, J., & Gao, Y. (2020). Development of food-grade bigels based on κ-carrageenan hydrogel and monoglyceride oleogels as carriers for β-carotene: Roles of oleogel fraction. *Food Hydrocolloids, 105*, Article 105855. https://doi.org/10.1016/j.foodhyd.2020.105855

Zhou, X., Jiang, S., Zhao, D., Zhang, J., Gu, S., Pan, Z., & Ding, Y. (2017). Changes in physicochemical properties and protein structure of surimi enhanced with camellia tea oil. *LWT, 84*, 562–571. https://doi.org/10.1016/j.lwt.2017.03.026